

Ab Initio Classical Trajectory Study of the Fragmentation of C₃H₄ Dications on the Singlet and Triplet Surfaces

Brian T. Psciuk, Peng Tao, and H. Bernhard Schlegel*

Department of Chemistry, Wayne State University, Detroit, Michigan 48202

Received: March 11, 2010; Revised Manuscript Received: June 11, 2010

Ab initio molecular dynamics have been used to examine the fragmentation of allene, propyne, and cyclopropene dications on the singlet and triplet potential energy surfaces. Accurate energies and barrier heights were computed at the CBS-APNO level of theory. Classical trajectories were calculated at the B3LYP/6-31G(d,p) level of theory. To simulate vertical double ionizations of allene, propyne, and cyclopropene by short, intense laser pulses, the trajectories were started from the corresponding neutral geometries and were given ca. 240 kcal/mol excess kinetic energy; 200 trajectories were integrated for each case. Approximately one-third of the trajectories underwent extensive rearrangement before dissociation. Proton dissociation is the dominant pathway for all six cases, accounting for 50–75% of the trajectories. H₂/H₂⁺ is produced in ca. 20% of the trajectories on the singlet propyne and cyclopropene dication surface. The calculated ratio of CH⁺/CH₂⁺/CH₃⁺ compares favorably to that obtained in laser-induced Coulomb explosion of allene. The yield of CH₂⁺ is ca. 12% on the singlet and triplet allene dication surfaces compared to 6% or less in the other cases, whereas CH⁺ is favored on the singlet propyne dication surface (12% vs 0–8% on the other surfaces). CH₃⁺ is formed primarily by direct dissociation on the triplet propyne dication surface (5% vs <1% on the other surfaces). The small amount of H₃⁺ seen experimentally for allene indicates that rearrangement can occur before dissociation. The dynamics simulations confirm that extensive isomerization occurs, even though the initial kinetic energy was too high to yield H₃⁺.

Introduction

Coulomb explosion is one of the processes that can occur when molecules are subject to intense laser fields.^{1–3} When a sufficient number of electrons are removed from a molecule, dissociation is spontaneous. For dications, however, dissociation is not necessarily spontaneous because enough electrons remain for significant bonding. Nevertheless, the barriers are diminished by the Coulombic repulsion. Thus, there may be an interesting interplay between energetics and dynamics in the fragmentation processes of dications.

Allene (H₂C=C=CH₂) was one of the first polyatomic molecules to be studied by laser induced Coulomb explosion.⁴ The dication of allene can be formed by interaction with short, intense laser pulses,^{4–7} by electron impact,⁸ and by double charge transfer.^{9–12} Dissociation of the dication yields a variety of charged fragments: C₃H_{*n*}²⁺, C₃H_{*n*}⁺, C₂H_{*n*}⁺, CH_{*n*}⁺, and H_{*n*}⁺ (*n* = 1–3).^{4–6,8} The Coulomb explosion of propyne (H₃C–C≡CH), an isomer of allene, yields a different pattern of intensities for the various fragments.⁸ Cyclopropene is another stable isomer of allene, but the dissociation of its dication has not been studied experimentally.

The potential energy surface for allene dication has been calculated by a number of investigators.^{13–16} The most recent study is a very thorough investigation of the singlet and triplet potential surfaces of C₃H₄²⁺ by Mebel and Bandrauk.¹³ Barriers for rearrangement and fragmentation were computed by density functional theory and coupled cluster methods. For cases suspected of having diradical character, structures and energies were also computed at the CASSCF and CASPT2 levels of

theory. Branching ratios for various fragmentation pathways were estimated by RRKM theory.

In previous studies, we have used ab initio molecular dynamics to investigate the dissociation of small ions.^{17,18} These studies showed that the fragmentation trajectories could be grouped into two categories: (1) direct, involving only a few vibrations before dissociation; and (2) indirect, involving one or more rearrangement steps before dissociation. Although some of the indirect trajectories pass through recognizable transition states, others explore higher energy regions of the potential surface before dissociating (see some of the movies in the Supporting Information). The latter is akin to the roaming mechanism for formaldehyde and acetaldehyde dissociation, which has been established both experimentally and theoretically.^{19–21}

Ionization by short intense laser pulses can deposit considerable amounts of energy in the ions, but statistical methods such as RRKM may not be valid at higher energies. However, trajectory calculations may be able to shed some light on the dissociation processes at higher energies. In the present paper, we used ab initio molecular dynamics to examine the fragmentation of C₃H₄²⁺ on both the singlet and triplet potential energy surfaces. Accurate energies and barrier heights were computed at the CBS-APNO²² level of theory and were compared to the extensive work by Mebel.¹³ Classical trajectories were calculated at the B3LYP/6-31G(d,p) level of theory since the energetics at this level of theory are in good agreement with more accurate methods. Experimental studies have shown a strong isomer effect on the fragmentation pattern of C₃H₄²⁺.⁸ To probe this computationally, trajectories were initiated at the neutral allene, propyne, and cyclopropene ground state geometries.

* To whom correspondence should be addressed.

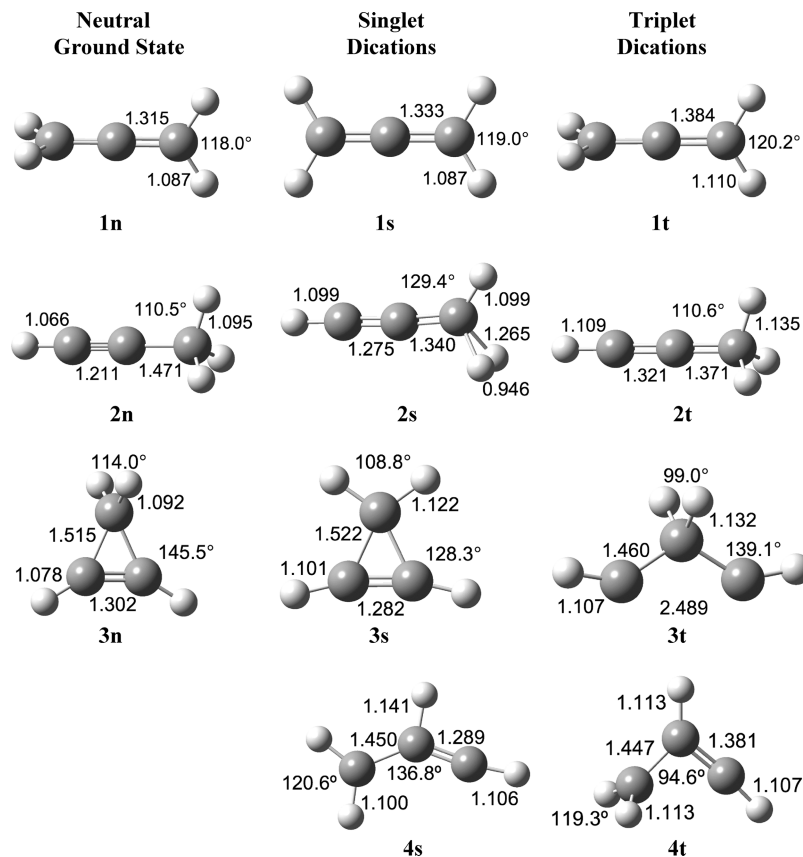


Figure 1. Geometries with relevant bond lengths (Å) and angles (°) for isomers on the ground neutral, singlet dication, and triplet dication state surfaces optimized at the QCISD/6-311G(d,p) level of theory.

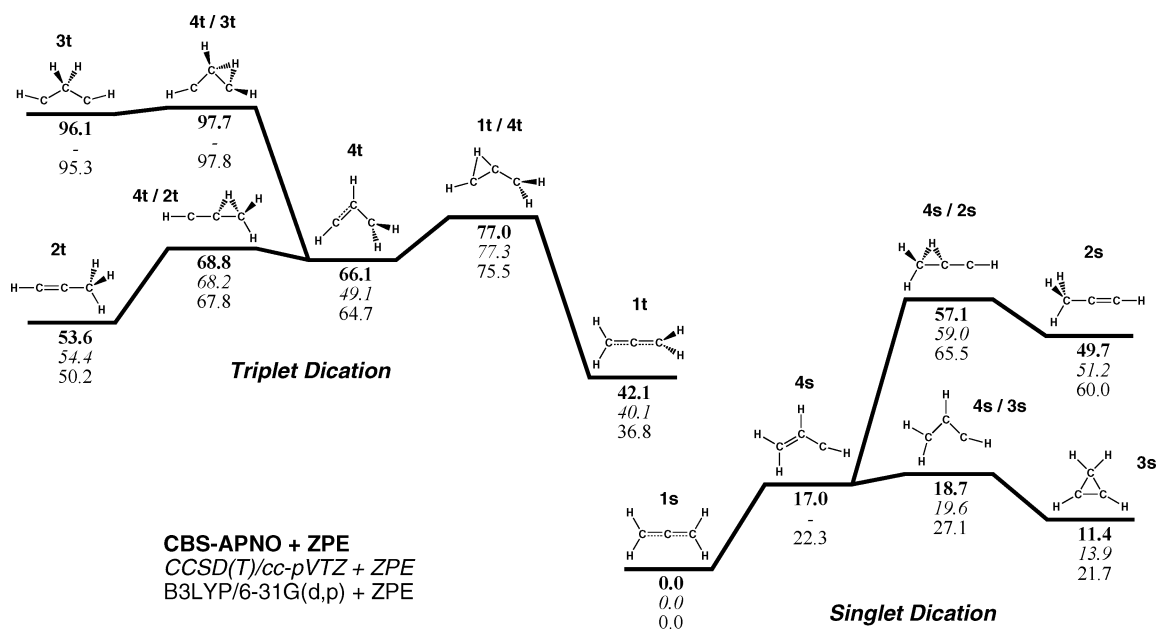


Figure 2. Potential energy surfaces for singlet and triplet $C_3H_4^{2+}$. Relative energies with zero point energy (kcal/mol) at the CBS-APNO (in bold), CCSD(T)/cc-pVTZ//B3LYP/6-311G(d,p) (in italics) and B3LYP/6-31G(d,p) levels of theory.

Methods

Electronic structure calculations were performed with the development version of the Gaussian software suite.²³ Geometries were optimized by density functional theory (DFT) using the B3LYP functional^{24,25} with the 6-31G(d,p) and 6-311G(d,p) basis sets^{26–29} and by quadratic configuration interaction³⁰ (QCISD) with the 6-311G(d,p) basis set. Vibrational frequencies were calculated at each level of theory to confirm that the

structures were either minima or transition states. Reaction path following in mass-weighted Cartesian coordinates was used to connect transition states to their corresponding minima.^{31,32} Relative energies were calculated with the B3LYP/6-31G(d,p), B3LYP/6-311G(d,p), and CBS-APNO²² levels of theory.

Ab initio molecular dynamics calculations were carried out using classical trajectories computed with a Hessian-based predictor–corrector method^{33,34} at the B3LYP/6-31G(d,p) level

TABLE 1: Calculated Adiabatic Double Ionization Energies (eV) for Allene, Propyne, and Cyclopropene

	B3LYP/ 6-31G(d,p)	B3LYP/ 6-311G(d,p)	CBS-APNO	CCSD(T)/ cc-pVTZ ^a
1n → 1s	25.30	25.55	25.93	25.84
1n → 1t	26.89	27.17	27.75	27.58
2n → 2s	27.77	28.00	28.13	28.08
2n → 2t	27.34	27.64	28.30	28.22
3n → 3s	25.17	25.35	25.43	
3n → 4t	27.04	27.27	27.80	

^a Reference 10.

of theory. A step size of 0.25 amu^{1/2} bohr was used, and the Hessians were updated for three molecular dynamics steps before being recalculated analytically; the angular forces were projected out for the corrector step. Sets of 200 trajectories were calculated for allene, propyne, and cyclopropene dications on the singlet and triplet potential energy surfaces starting from the geometry of the neutral ground state singlet. A fixed amount of kinetic energy (190–240 kcal/mol) was added to the initial structure. Initial momenta for the nuclei were chosen by using orthant sampling³⁵ to allocate this kinetic energy. To simulate vertical ionizations, the initial positions of the nuclei were not displaced from their neutral ground state geometry. At each step in a trajectory, the SCF calculation was started with an unrestricted initial guess (using the GUESS=MIX keyword in

Gaussian for singlet trajectories) to permit homolytic bond dissociation. For most trajectories, the energy was conserved to better than 1×10^{-5} hartree and the angular momentum was conserved to $1 \times 10^{-8} \hbar$. Only a few trajectories had to be discarded due to a significant fluctuation in the total energy before reaching a transition state for dissociation. Trajectories were integrated for a maximum of 600 steps (approximately 250 fs) and were terminated if the distance between the centers of mass of the fragments exceeded 12.0 bohr.

Results and Discussion

Structures and Energetics. Selected geometries on the C₃H₄ neutral and dication potential energy surfaces are shown in Figure 1. For allene, double ionization increases the CC bond length as expected. The singlet dication, **1s**, is planar to maximize the remaining π bonding, whereas in the triplet dication, **1t**, the two CH₂ groups are perpendicular similar to the neutral ground state. Formation of triplet propyne dication, **2t**, results in elongation of the triple bond and shortening of the single bond. The singlet propyne dication, **2s**, begins to look like HCCCH²⁺·H₂, with two of the CH bonds elongated to 1.27 Å and the associated HH distance shortened to 0.95 Å. In cyclopropene singlet dication, **3s**, two electrons are removed from the π bond and the CH₂ group rotates into the plane in order to increase the π bonding. Excitation of singlet cyclopropene dication to the triplet promotes an electron from a CC

TABLE 2: Relative Energies of Optimized C₃H₄²⁺ Surface Stationary Points for Singlet and Triplet States (kcal/mol)

	B3LYP/ 6-31G(d,p)	B3LYP/ 6-311G(d,p)	CBS-APNO	CBS-APNO+ZPE	CCSD(T)/ cc-pVTZ+ZPE ^a
1s	0.0	0.0	0.0	0.0	0.0
TS 1s/H⁺ + H₂CCCH⁺	83.8	81.8	85.7	80.8	82.0
H⁺ + H₂CCCH⁺	20.8	18.1	10.7	5.9	8.5
TS 1s/CH₂⁺ + H₂CC⁺	127.5	127.7	128.6 ^b	124.0 ^b	114.7 ^c
CH₂⁺ + H₂CC⁺	59.3	59.0	55.3	48.5	46.7
TS 1s/4s	22.1	21.4 ^d	15.4	14.6	
4s	22.0	21.6 ^d	16.3	17.0	
TS 4s/CH⁺ + H₂CCH⁺	117.5	117.0	111.3	107.7	104.2
CH⁺ + H₂CCH⁺	34.4	32.4	19.5	14.2	11.0
TS 4s/3s	26.5	26.2	18.6	18.7	19.6
3s	21.9	21.4	12.6	11.4	13.9
TS 3s/H⁺ + c-C₃H₃⁺	75.4	74.6	72.4	67.2	69.6
H⁺ + c-C₃H₃⁺	-6.2	-7.3	-17.7	-20.9	-18.4
TS 4s/2s	68.5	67.1	60.4	57.1	59.0
2s	61.8	60.0	51.3	49.7	51.2
TS 2s/CH₃⁺ + C₂H⁺	117.2	117.7	114.7 ^b	112.8 ^b	124.1 ^e
CH₃⁺ + C₂H⁺	66.8	66.6	57.8	54.1	80.9 ^e
1t	36.8	37.4	41.5	42.1	(40.1)
TS 1t/H⁺ + H₂CCCH⁺	97.2	96.0	112.2 ^b	105.4 ^b	105.6
H⁺ + H₂CCCH⁺	58.5	56.7	55.3	47.4	49.8
TS 1t/4t	80.0	79.1	81.8	77.0	77.3
4t	66.0	66.6	68.1	66.1	49.1 ^f
TS 4t/H⁺ + c-C₃H₃⁺	117.4	116.2	121.2 ^b	113.8 ^b	114.5
H⁺ + c-C₃H₃⁺	86.4	85.0	80.3	72.0	74.3
TS 4t/CH₂⁺ + HCCH⁺	107.5	107.0	106.5	103.1	100.8
CH₂⁺ + HCCH⁺	17.3	15.4	11.9	5.9	4.4
TS 4t/3t	102.2	101.7	101.7	97.7	
3t	97.9	98.9	98.3	96.1	
TS 4t/2t	70.7	70.4	71.4	68.8	68.2
2t	52.6	52.4	55.5	53.6	54.4
TS 2t/H⁺ + H₂CCCH⁺	95.5	94.2	111.0 ^b	104.5 ^b	104.7
H⁺ + H₂CCCH⁺	58.5	56.7	55.3	47.4	49.8
MAD	5.8^g	5.4^g			1.7^h

^a Reference 10. ^b CBS-APNO energy using the B3LYP/6-311G(d,p) geometry. ^c CASPT2(8,8)/cc-pVTZ//CASSCF(8,8)/6-311G(d,p). ^d Single point energy using the B3LYP/6-31G(d,p) geometry. ^e Not included in the MAD (lower electronic state found). ^f Not included in the MAD (unable to produce this state). ^g Mean absolute deviation with respect to CBS-APNO. ^h Mean absolute deviation with respect to CBS-APNO+ZPE.

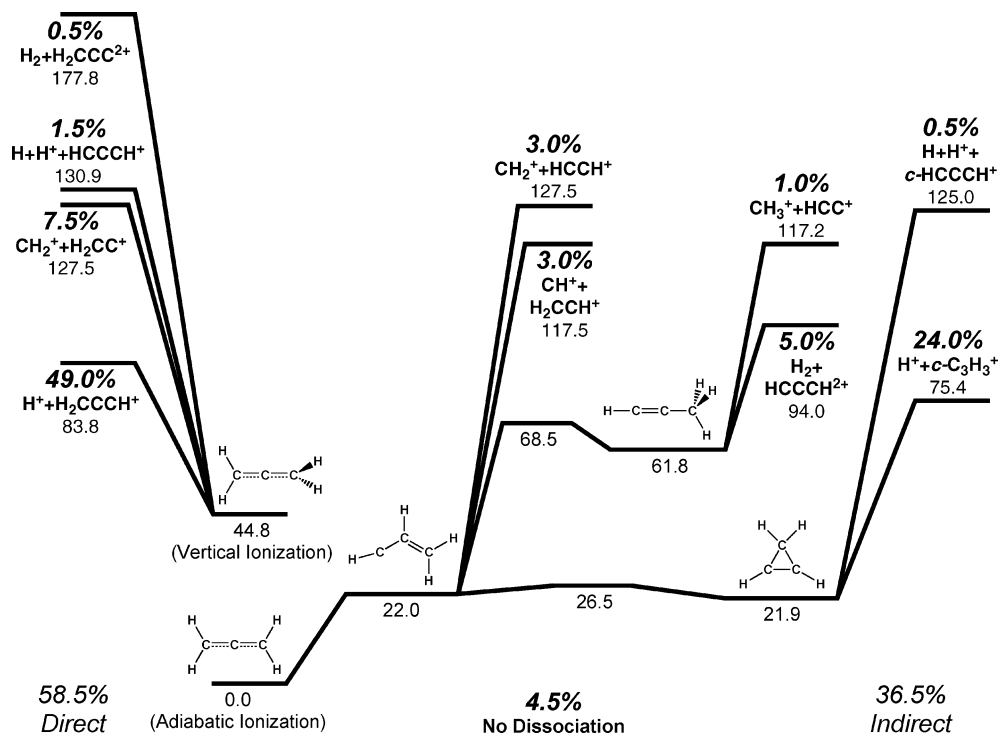


Figure 3. Fragmentation of vertically doubly ionized allene on the singlet surface. Left hand side shows the percentages and barriers for direct dissociation. Right hand side shows only the lowest barriers for indirect dissociation; percentages also include fragmentations occurring via higher barriers (199 trajectories calculated at the B3LYP/6-31G(d,p) level of theory with 240 kcal/mol initial kinetic energy).

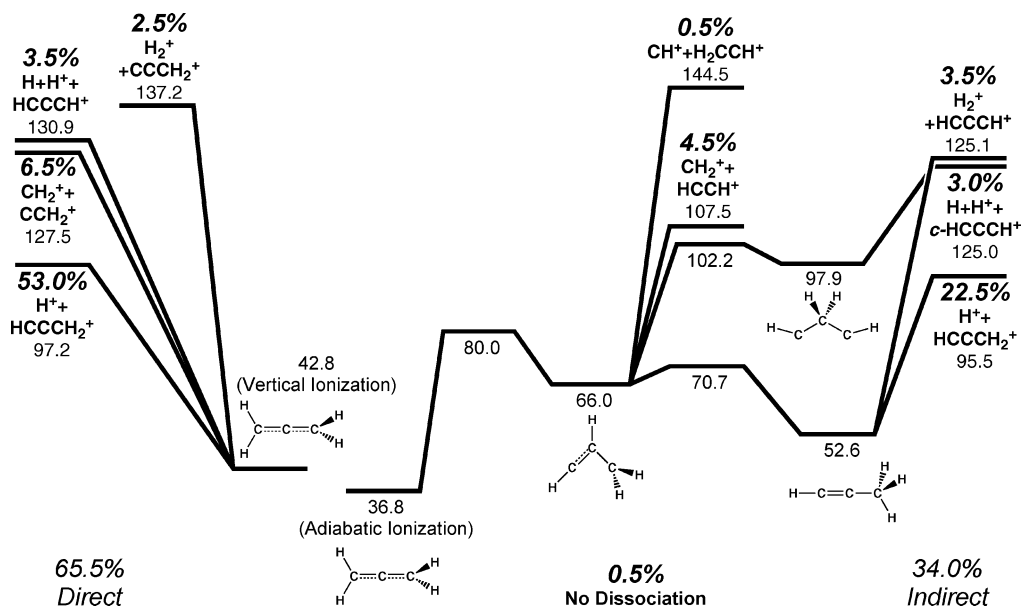


Figure 4. Fragmentation of vertically doubly ionized allene on the triplet surface. Left hand side shows the percentages and barriers for direct dissociation. Right hand side shows only the lowest barriers for indirect dissociation; percentages also include fragmentations occurring via higher barriers (200 trajectories calculated at the B3LYP/6-31G(d,p) level of theory with 240 kcal/mol initial kinetic energy).

σ bonding orbital to a σ^* antibonding orbital, breaking a CC bond and opening the ring. Depending on which CC bond is broken, this results in triplet methylene dicarbene dication, **3t**, or triplet vinylmethylene dication, **4t**. Vinylmethylene, **4t**, is also an intermediate in the conversion of allene to propyne on the triplet dication surface. However, on the singlet dication surface, vinylmethylene, **4s**, is only a very shallow minimum or a flat region of the potential energy surface on the pathway from allene to cyclopropene.

The relative energies calculated at the CBS-APNO level of theory are summarized in Figure 2 for the singlet and triplet

$C_3H_4^{2+}$ dications. Singlet allene, **1s**, is the most stable dication. A 1,2 hydrogen migration leads to the vinylmethylene structure, **4s**, which is 16 kcal/mol higher than **1s**. There is little or no barrier for this structure to return to **1s**, and only a small barrier exists for conversion to cyclopropene dication, **3s**. Singlet propyne dication, **2s**, is 51 kcal/mol higher than allene and is connected by a low barrier to the vinylmethylene dication, **4s**. Triplet allene dication, **1t**, is 41 kcal/mol higher in energy than the singlet and is the lowest energy structure on the triplet surface. A 1,2 hydrogen shift leads to the triplet vinylmethylene dication, **4t**, which is separated by small barriers from the allene

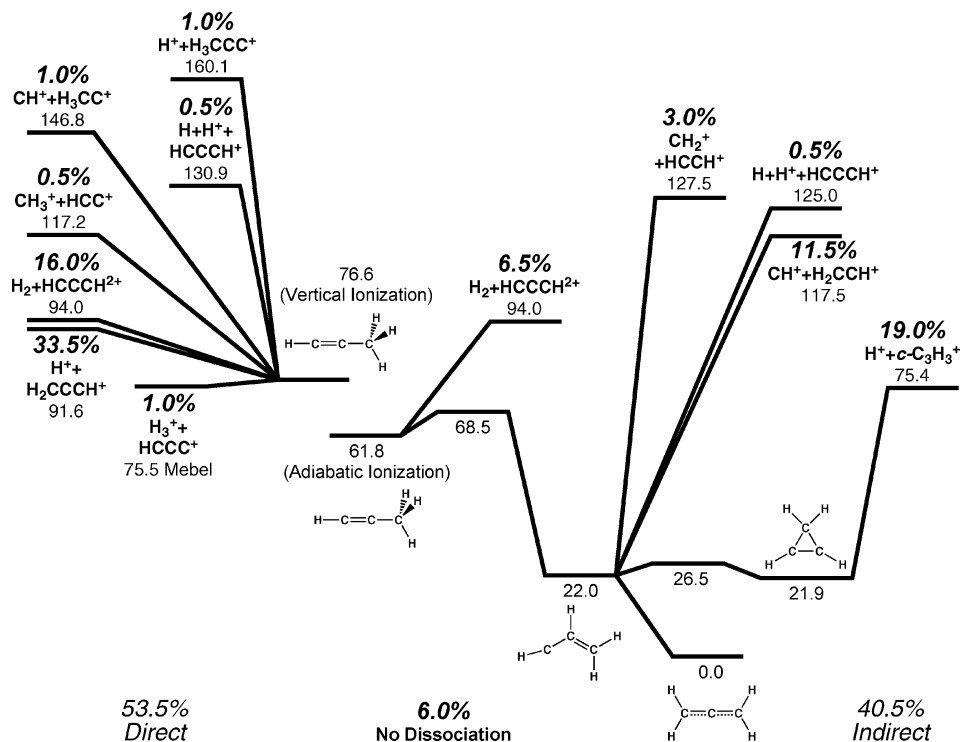


Figure 5. Fragmentation of vertically doubly ionized propyne on the singlet surface. Left hand side shows the percentages and barriers for direct dissociation. Right hand side shows only the lowest barriers for indirect dissociation; percentages also include fragmentations occurring via higher barriers (200 trajectories calculated at the B3LYP/6-31G(d,p) level of theory with 210 kcal/mol initial kinetic energy).

and propyne isomers. Triplet methylene dicarbene dication, **3t**, has a very low barrier for conversion to vinylmethylene, **4t**.

The adiabatic double ionization energies are listed in Table 1. The CBS-APNO values are 0.2–0.3 eV higher than Mebel's results.¹³ Table 2 compares the relative energies for key structures and transition states calculated by B3LYP/6-31G(d,p) and B3LYP/6-311G(d,p) with our CBS-APNO values and Mebel's CCSD(T)/cc-pVTZ results.¹³ With two exceptions, the CBS-APNO results agree very well with Mebel's data, with a mean absolute deviation of 1.7 kcal/mol. The mean absolute deviations for the B3LYP/6-31G(d,p) and B3LYP/6-311G(d,p) data compared to the CBS-APNO values are 5.8 and 5.4 kcal/mol, respectively. Since both sets of DFT calculations compare well with CBS-APNO calculations, the less expensive B3LYP/6-31G(d,p) level of theory was chosen for the ab initio molecular dynamics calculations.

Dynamics of the Dication Fragmentation. To simulate the fragmentation of the dications formed by vertical double ionization, the ab initio molecular dynamics calculations on the dication surfaces were initiated from the neutral ground state geometries. Since experimental studies found a significant isomer dependence of the fragmentation pattern,⁸ the trajectories were started from the three stable structures of C₃H₄: allene, propyne, and cyclopropene. The fragmentation patterns also indicate that considerable rearrangement can occur before dissociation. Ionization by a short intense laser pulse can impart a considerable amount of energy to the resulting ions. Since no suitable estimate is available for the range of energies, somewhat arbitrary choices need to be made. As a matter of practicality for the computational simulation, the ions should have enough excess kinetic energy so that most dissociate in a relatively short time. With too much extra energy, the ions fragment before having a chance to rearrange; with too little energy, the dominant influence is the barrier height rather than the molecular dynamics. After some experimentation with singlet allene

dication, we found that with 240 kcal/mol kinetic energy ca. 95% of the trajectories dissociated within the 250 fs simulation time, and about half of the trajectories involved rearrangements. Since the vertically ionized singlet propyne and cyclopropene dications are 32 and 40 kcal/mol above the vertically ionized singlet allene dication, these trajectories were started with 210 and 200 kcal/mol of kinetic energy, respectively, so as to keep the total energy approximately constant. Relative to the vertically ionized singlet allene dication, energies of the vertically ionized triplet allene, propyne, and cyclopropene dications are –2, 26, and 45 kcal/mol, respectively; these were started with 240, 210, and 190 kcal/mol of kinetic energy, respectively. Since the triplet allene and propyne dication geometries are fairly close to the neutral geometries (see Figure 1), these vertically ionized triplet dications are only 6 and 18 kcal/mol higher than their equilibrium structures. By contrast, the methylene groups in singlet allene and cyclopropene dication are twisted by 90° compared to the neutral ground state geometries, and these vertically ionized singlet dications are 45 and 63 kcal/mol higher than the corresponding equilibrium structures. Vertically excited triplet cyclopropene dication is a saddlepoint and opens to vinylmethylene, **4t**, rather than methylene dicarbene, **3t**.

For singlet and triplet allene, propyne, and cyclopropene dication, 200 trajectories were calculated for maximum of ca. 250 fs. The results of the ab initio molecular dynamics simulations are summarized in Figures 3–8. Movies of selected trajectories are available in the Supporting Information. The figures show the initial vertically excited dications and the adiabatic dication structures, the various intermediates, and the dissociation channels. The trajectories can be grouped into two categories: direct and indirect. Direct trajectories proceed to products without rearrangement. Several vibrations may occur before the ion passes over the barrier, but the ion stays in the same valley that it started in. Indirect trajectories pass through one or more intermediates before dissociation. Direct processes

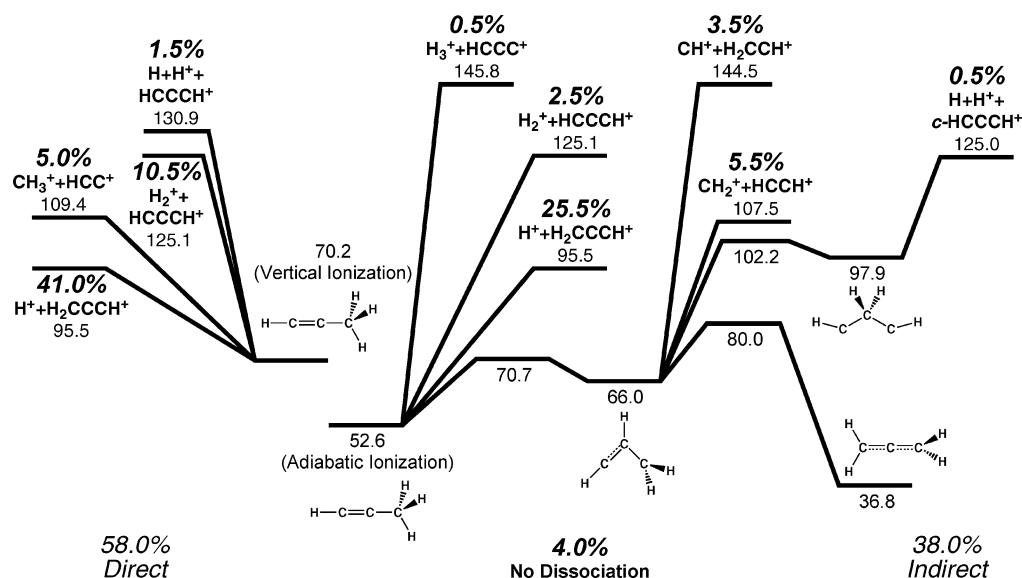


Figure 6. Fragmentation of vertically doubly ionized propyne on the triplet surface. Left hand side shows the percentages and barriers for direct dissociation. Right hand side shows only the lowest barriers for indirect dissociation; percentages also include fragmentations occurring via higher barriers (200 trajectories calculated at the B3LYP/6-31G(d,p) level of theory with 210 kcal/mol initial kinetic energy).

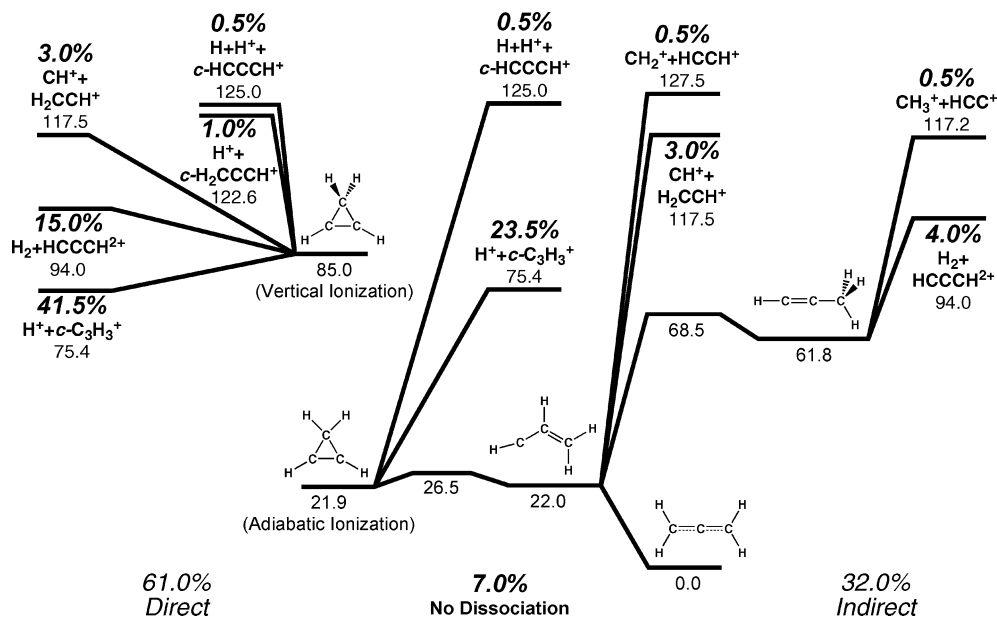


Figure 7. Fragmentation of vertically doubly ionized cyclopropene on the singlet surface. Left hand side shows the percentages and barriers for direct dissociation. Right hand side shows only the lowest barriers for indirect dissociation; percentages also include fragmentations occurring via higher barriers (200 trajectories calculated at the B3LYP/6-31G(d,p) level of theory with 200 kcal/mol initial kinetic energy).

and their barrier heights are shown on the left-hand side of Figures 3–8. For about half of the trajectories, there is considerable rearrangement before dissociation. These indirect trajectories are shown on the right-hand side of Figures 3–8. Because of the large amplitude motions, it is often difficult to assign a trajectory to a particular transition state (see some of the movies in the Supporting Information). The dissociating trajectories are classified according to the lowest energy transition state leading to the observed product. The percentages for each indirect product also include fragmentations that occur via higher energy barriers leading to the same products.

For the selected initial energy, the average dissociation time is ca. 90 fs, with 90% of the trajectories completing in ca. 190 fs. Direct dissociation of H^+ is the fastest event, having an average time of 45–50 fs, with 90% completing within ca. 75 fs. Direct dissociations other than H^+ take

approximately twice as long, in part because the fragments are heavier and require more time to separate. Indirect dissociation trajectories involve significant rearrangement and are 2–3 times longer than direct trajectories, averaging ca. 145 fs versus ca. 55 fs for direct dissociation. There is no significant difference for the average dissociation times for the singlets versus the triplets; likewise, the average times for allene, propyne, and cyclopropene are very similar. (For details see Table S2 of the Supporting Information).

Deprotonation is the dominant fragmentation process for all six sets of trajectories, ranging from 54 to 76% of the trajectories. Each set of trajectories displayed a ratio of ca. 2:1 between direct and indirect deprotonation. The ratios of the other fragmentation products varied considerably with the starting structure and spin state of the dication.

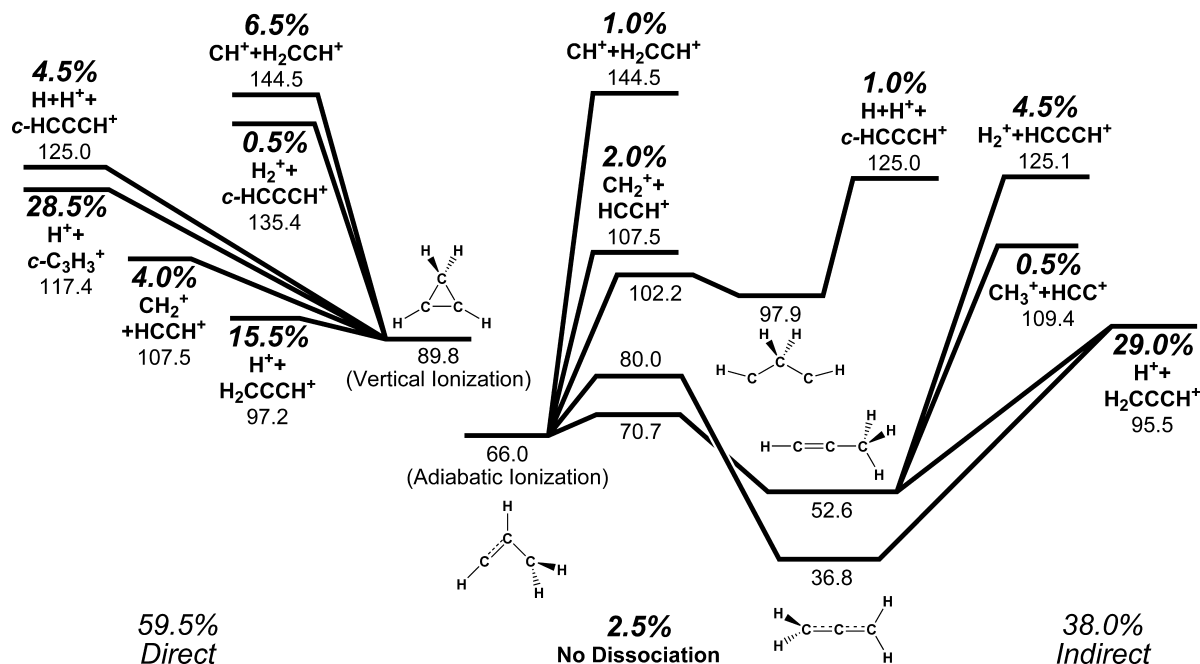


Figure 8. Fragmentation of vertically doubly ionized cyclopropene on the triplet surface. Left hand side shows the percentages and barriers for direct dissociation. Right hand side shows only the lowest barriers for indirect dissociation; percentages also include fragmentation occurring via higher barriers (200 trajectories calculated at the B3LYP/6-31G(d,p) level of theory with 190 kcal/mol initial kinetic energy).

For the direct dissociations, the largest percentages of products were formed via the lowest energy barriers. One exception is H₃⁺ + CCCH on the singlet propyne dication surface that is formed by dissociation of H₂ followed by abstraction of H⁺ by H₂ as described by Mebel and Bandrauk.¹³ For the large excess kinetic energies used in the present study, H₂ dissociates with considerable energy and is less likely to return and abstract a proton. Other exceptions include the H₂⁺ + c-HCCCH channel on the triplet propyne dication surface and the CH⁺ + H₂CCH⁺ channel on the triplet cyclopropene dication surface.

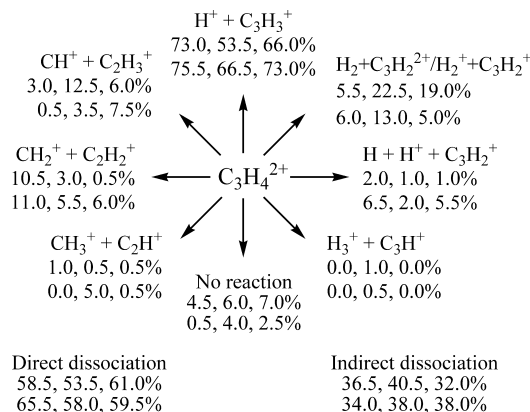
For the indirect dissociations, the channels with the lowest barriers also had the highest percentage of products. In cases where the final barriers are similar, higher percentages are found for processes going through the fewest intermediates or lowest intermediate barriers. Even though some of the indirect dissociation barriers are lower than the corresponding direct barriers, the percentage of indirect product was lower because of the need for rearrangement. The high yield for H⁺ + H₂CCCH⁺ on the triplet cyclopropene dication surface is the result of ring-opening to vinylmethylene which has a large driving force for rearrangement to propyne and allene dications, which both dissociate to H⁺ + H₂CCCH.

A number of the trajectories dissociated into three fragments, for example, H + H⁺ + C₃H₂⁺. For these cases, the two C–H bonds broke in quick succession. Additional three-body fragmentations can occur in a stepwise process by subsequent dissociation of the initial two-body fragmentation products. Because the fragment ions possess a large excess of kinetic energy, such fragmentation can happen readily. However, the stopping criteria for the trajectories were chosen to count only the first dissociation event.

Summary

Ab initio molecular dynamics have been used to examine the fragmentation of singlet and triplet allene, propyne, and cyclopropene dications. To simulate vertical excitation by short, intense laser pulses, the trajectories were started from the

SCHEME 1: Percentages of Initial Dissociation Products from the Fragmentation of C₃H₄²⁺ on the Singlet Surface (Top Row) and Triplet Surface (Bottom Row), Starting from Allene, Propyne, and Cyclopropene, Respectively



corresponding neutral geometries and were given ca. 240 kcal/mol excess kinetic energy relative to the singlet allene dication. The fragmentation patterns are summarized in Scheme 1. Although the specific percentages for various products will depend on the amount of the excess kinetic energy, some of the trends may be less sensitive to the initial conditions. Internal rearrangement can occur quite readily in the dications, and the ratio of direct to indirect dissociation is ca. 2:1 at this energy. In agreement with experiments on allene and propyne,^{4–8} deprotonation to give H⁺ + C₃H₃⁺ is calculated to be the dominant pathway, and that for H₂⁺ + C₂H₂⁺ is a factor of 5–10 lower. The yield of H₂/H₂⁺ is highest on the singlet propyne and cyclopropene dication surface. For the allene dication, the calculated ratio of CH₂⁺ ≫ CH⁺ > CH₃⁺ is in good accord with ion coincidence measurements of laser induced Coulomb explosion (1:0.08:0.03).⁶ The highest yield of CH₃⁺ is by direct dissociation on the triplet propyne surface. Production of CH₂⁺ is more favorable on the singlet and triplet allene dication surfaces, whereas CH⁺ is favored on the singlet propyne dication

surface. In experiments on allene,⁶ a small amount of H₃⁺ was produced and was taken as evidence that isomerization could occur before dissociation. The classical trajectory calculations confirm that extensive rearrangement occurs in conjunction with dissociation, although H₃⁺ is not produced at the higher initial kinetic energies used in the present study.

Acknowledgment. This work was supported by grant No. CHE0910858 from the National Science Foundation. Computer time on Wayne State University computer grid is gratefully acknowledged.

Supporting Information Available: Geometries for allene, propyne, and cyclopropene neutral, singlet dication, and triplet dication optimized at QCISD/6-311G(d,p), timing data for the trajectories, structures for the product fragments, and movies of selected trajectories. This material is available free of charge via the Internet at <http://pubs.acs.org>.

References and Notes

- (1) Posthumus, J. H. *Rep. Prog. Phys.* **2004**, *67*, 623.
- (2) Corkum, P. B.; Ivanov, M. Y.; Wright, J. S. *Annu. Rev. Phys. Chem.* **1997**, *48*, 387.
- (3) Sheehy, B.; DiMauro, L. F. *Annu. Rev. Phys. Chem.* **1996**, *47*, 463.
- (4) Cornaggia, C. *Phys. Rev. A* **1995**, *52*, 4328.
- (5) Xu, H. L.; Okino, T.; Yamanouchi, K. *J. Chem. Phys.* **2009**, *131*, 151102.
- (6) Xu, H.; Okino, T.; Yamanouchi, K. *Chem. Phys. Lett.* **2009**, *469*, 255.
- (7) Hoshina, K.; Furukawa, Y.; Okino, T.; Yamanouchi, K. *J. Chem. Phys.* **2008**, *129*, 104302.
- (8) Scully, S. W. J.; Senthil, V.; Wyer, J. A.; Shah, M. B.; Montenegro, E. C.; Kimura, M.; Tawara, H. *Phys. Rev. A* **2005**, *72*, 030701.
- (9) Andrews, S. R.; Parry, D. E.; Harris, F. M. *J. Chem. Soc., Faraday Trans.* **1995**, *91*, 1181.
- (10) Andrews, S. R.; Parry, D. E.; Vairamani, M.; Harris, F. M. *J. Chem. Soc., Faraday Trans.* **1992**, *88*, 3403.
- (11) Andrews, S. R.; Harris, F. M.; Parry, D. E. *Chem. Phys.* **1995**, *194*, 215.
- (12) Jeffreys, N.; Parry, D. E.; Harris, F. M. *J. Chem. Soc., Faraday Trans.* **1998**, *94*, 1561.
- (13) Mebel, A. M.; Bandrauk, A. D. *J. Chem. Phys.* **2008**, *129*, 224311.
- (14) Lammertsma, K.; Schleyer, P. V. *J. Am. Chem. Soc.* **1990**, *112*, 7935.
- (15) Wong, M. W.; Radom, L. *J. Mol. Struct.* **1989**, *198*, 391.
- (16) Frenking, G.; Schwarz, H. *Int. J. Mass Spectrom. Ion Process.* **1983**, *52*, 131.
- (17) Zhou, J.; Schlegel, H. B. *J. Phys. Chem. A* **2009**, *113*, 9958.
- (18) Li, X. S.; Schlegel, H. B. *J. Phys. Chem. A* **2004**, *108*, 468.
- (19) Suits, A. G. *Acc. Chem. Res.* **2008**, *41*, 873.
- (20) Lahankar, S. A.; Chambreau, S. D.; Townsend, D.; Suits, F.; Farnum, J.; Zhang, X. B.; Bowman, J. M.; Suits, A. G. *J. Chem. Phys.* **2006**, *125*, 044303.
- (21) Townsend, D.; Lahankar, S. A.; Lee, S. K.; Chambreau, S. D.; Suits, A. G.; Zhang, X.; Rheinecker, J.; Harding, L. B.; Bowman, J. M. *Science* **2004**, *306*, 1158.
- (22) Ochterski, J. W.; Petersson, G. A.; Montgomery, J. A. *J. Chem. Phys.* **1996**, *104*, 2598.
- (23) Frisch, M. J.; Trucks, G. W.; Schlegel, H. B.; Scuseria, G. E.; Robb, M. A.; Cheeseman, J. R.; Scalmani, G.; Barone, V.; Mennucci, B.; Petersson, G. A.; Nakatsuji, H.; Caricato, M.; Li, X.; Hratchian, H. P.; Izmaylov, A. F.; Bloino, J.; Zheng, G.; Sonnenberg, J. L.; Hada, M.; Ehara, M.; Toyota, K.; Fukuda, R.; Hasegawa, J.; Ishida, M.; Nakajima, T.; Honda, Y.; Kitao, O.; Nakai, H.; Vreven, T.; Montgomery, J. A.; Peralta, J. E.; Ogliaro, F.; Bearpark, M.; Heyd, J. J.; Brothers, E.; Kudin, K. N.; Staroverov, V. N.; Kobayashi, R.; Normand, J.; Raghavachari, K.; Rendell, A.; Burant, J. C.; Iyengar, S. S.; Tomasi, J.; Cossi, M.; Rega, N.; Millam, J. M.; Klene, M.; Knox, J. E.; Cross, J. B.; Bakken, V.; Adamo, C.; Jaramillo, J.; Gomperts, R.; Stratmann, R. E.; Yazyev, O.; Austin, A. J.; Cammi, R.; Pomelli, C.; Ochterski, J. W.; Salvador, P.; Dannenberg, J. J.; Dapprich, S.; Parandekar, P. V.; Mayhall, N. J.; Daniels, A. D.; Farkas, O.; Foresman, J. B.; Ortiz, J. V.; Cioslowski, J.; Fox, D. J. *Gaussian Development Version, Revision H.X4*; Gaussian, Inc.: Wallingford, CT, 2009.
- (24) Becke, A. D. *J. Chem. Phys.* **1993**, *98*, 5648.
- (25) Lee, C. T.; Yang, W. T.; Parr, R. G. *Phys. Rev. B* **1988**, *37*, 785.
- (26) Krishnan, R.; Binkley, J. S.; Seeger, R.; Pople, J. A. *J. Chem. Phys.* **1980**, *72*, 650.
- (27) Hariharan, P. C.; Pople, J. A. *Theor. Chem. Acc.* **1973**, *28*, 213.
- (28) Hehre, W. J.; Ditchfield, R.; Pople, J. A. *J. Chem. Phys.* **1972**, *56*, 2257.
- (29) Ditchfield, R.; Hehre, W. J.; Pople, J. A. *J. Chem. Phys.* **1971**, *54*, 724.
- (30) Pople, J. A.; Head-Gordon, M.; Raghavachari, K. *J. Chem. Phys.* **1987**, *87*, 5968.
- (31) Hratchian, H. P.; Schlegel, H. B. *J. Chem. Theory Comput.* **2005**, *1*, 61.
- (32) Hratchian, H. P.; Schlegel, H. B. *J. Chem. Phys.* **2004**, *120*, 9918.
- (33) Millam, J. M.; Bakken, V.; Chen, W.; Hase, W. L.; Schlegel, H. B. *J. Chem. Phys.* **1999**, *111*, 3800.
- (34) Bakken, V.; Millam, J. M.; Schlegel, H. B. *J. Chem. Phys.* **1999**, *111*, 8773.
- (35) Bunker, D. L.; Hase, W. L. *J. Chem. Phys.* **1973**, *59*, 4621.

JP102238G